

How Does the Onset of Offset Influence Geologic Slip Rates?

Alexandra E. Hatem^{*1} , Richard W. Briggs¹ , and Ryan D. Gold¹ 

Abstract

Geologic slip rates are typically based on the displacement accrued by a geomorphic or stratigraphic feature and the age of the offset feature. Because slip rates are commonly calculated by dividing the displacement of a faulted marker by its age, they contain two open time intervals: the elapsed time between the age of an offset feature and the age of the earthquake that displaced the feature, and the time between the present-day and the most recent earthquake. Here, we explore the influence of including unconstrained open intervals in geologic slip rate calculations. We test the degree to which these open intervals affect geologic slip rates and their uncertainties, and we find that their influence depends primarily on mean earthquake recurrence intervals (RIs). Slip rates on faults with longer RIs, such as the Wasatch fault, can be greatly influenced by an increase of up to 20% when accounting for open intervals. In contrast, slip rates on faults with shorter RIs, such as the San Andreas fault, are only slightly influenced by the assumption that slip rates calculated over open intervals approximate those calculated over closed intervals. Our analyses indicate that faults with moderate slip rates ($\sim 0.2\text{--}5 \text{ mm/yr}$) are sensitive to both open interval effects themselves, as well as methods to quantify and account for these effects. We re-evaluate how slip rates are calculated and defined in displacement-time space using published deformation records. We explore the utility of assigning a probability distribution to the initiation of offset of the oldest faulted feature and the timing of the most recent earthquake (MRE). We find that calculating geologic slip rates without using probability distributions that capture the timing of the MRE and the onset of offset of the oldest faulted feature, especially on slow-to-moderate slip rate faults, can lead to systematic underestimation of average geologic slip rates.

Cite this article as Hatem, A. E., R. W. Briggs, and R. D. Gold (2024). How Does the Onset of Offset Influence Geologic Slip Rates? *Seismol. Res. Lett.* **96**, 363–376, doi: [10.1785/0220240096](https://doi.org/10.1785/0220240096).

Introduction

Geologic slip rates are defined as the displacement on a fault divided by the time over which that displacement has accrued (e.g., Wallace, 1946; McGill and Sieh, 1993; Central and Eastern United States Seismic Source Characterization for Nuclear Facilities [CEUS-SSCn], 2012). The time over which displacement accumulates is commonly assumed to be the elapsed time between the age of an offset feature and the present (i.e., the age of the faulted feature). This time interval is typically assumed to include multiple earthquakes, and a geologic slip rate approximates the average rate of displacement over an unknown number of earthquakes.

Implicit in typical slip rate calculations is the assumption that the time interval over which a geologic feature is displaced is bounded by earthquakes. In practice, this assumption is rarely true because the age of bounding earthquakes is usually not explicitly incorporated. Paleoseismic investigations may be able to define the timing of the most recent earthquake (MREs) for slip rate calculations, but most faults do not have a documented paleoseismic history. For example, in the State of

California, the best-studied state with the fastest slipping faults in the conterminous United States, ~ 40 faults have paleoseismic investigations (Weldon *et al.*, 2013; McPhillips, 2022) and ~ 150 faults have field observed estimates of geologic slip rates (Dawson and Weldon, 2013; Hatem *et al.*, 2022) out of ~ 350 faults considered causative faults for damaging earthquakes. Even in the best-studied region along the Pacific-North American plate boundary, our view of fault history is spatially and temporally incomplete and is usually limited to geologic slip rate sites typically unrelated to paleoseismic sites or the earthquakes these slip rates attempt to constrain.

In the absence of paleoseismic records for most faults, we propose that geologic slip rate estimates can be improved by estimating the timing of earthquakes that bound a geologic slip

1. U.S. Geological Survey, Geologic Hazards Science Center, Golden, Colorado, U.S.A.,  <https://orcid.org/0000-0001-7584-2235> (AEH);  <https://orcid.org/0000-0002-4464-6394> (RDG)

*Corresponding author: ahatem@usgs.gov

© Seismological Society of America

rate. In our study, we refer to these bounding earthquakes as “anchors” because these are the earthquakes that define the slip rate time interval on either end (Fig. 1). For nearly all cases, we do not know the “onset of offset” or the timing of displacement. The term “open interval” is often used to refer to the elapsed time since the MRE, but the lag between the formation and offset of a faulted geologic feature—the onset of offset—is also an open interval that is usually ignored in slip rate calculations. An ideal geologic slip rate calculation will include only closed intervals by accounting for the onset of offset, or both open intervals, at each end of a time-displacement history.

The challenge we address is how to best estimate the age of the slip rate anchors to constrain the onset of offset. In the absence of a paleoseismic record, we usually rely exclusively on our knowledge of the displacement of the dated landform (Fig. 1a). However, neither the present-day nor the age of the dated offset feature represent anchors or bounding earthquakes in time-displacement space (Fig. 1b). Rather, they represent a location in time between two earthquakes. Instead of using the arbitrary points in time represented by the age of the offset feature and the present day, we explore possibilities to constrain the onset of offset for anchor earthquakes in geologic slip rate calculations (Fig. 1c).

Because a geologic slip rate ought to be bound over a discrete interval of time or a closed interval, we attempt to limit our slip rate calculation to the elapsed time between the estimated timing of two earthquakes. We schematically highlight a portion of this earthquake path as stairsteps in Figure 1c, with the earthquakes bounding this discrete time period (anchors). In an ideal scenario, anchors coincide exactly with the MRE timing and the oldest earthquake timing in a time-displacement history. In practice, anchors that bound time-displacement histories are rarely centered on earthquake occurrences, and so slip rate calculations commonly incorporate temporal open intervals at their youngest and oldest ends.

We focus on temporally closed interval slip rates—shown with dashed lines in Figure 1c—anchedored by earthquakes at their youngest and oldest extents. Traditional slip rate calculations (Fig. 1a) focus on cumulative displacement, or the starting and ending positions of the displaced landform, indicated by the dashed line connecting the white circle and white star in Figure 1c along an arbitrary set of steps that represent interseismic intervals and single-earthquake displacements. In this study, our investigation is centered on understanding the effect of earthquake timing, rather than displacement, on geologic slip rates. As such, we assume the following: (1) practitioners do not know displacement in the MRE or the first displacement value of the offset landform, (2) a single-earthquake displacement is a small increment of overall displacement, and (3) coseismic displacement and the preservation of such displacements are highly variable along a given rupture length. If items (1) or (2) are not true, our approach can be improved by accounting for first or last displacement values if they are

available. Additional probabilistic modeling may eventually account for item (3). For moderate-to-fast slipping faults, accounting for open intervals is likely more important than correcting for displacement. An outcome of the approach we outline here is that slip rates that approximate the timing of anchor earthquakes are consistently faster than conventionally derived slip rates, and the total elapsed time is shorter.

When does offset begin to accrue?

Because the relationship between the age of the faulted feature and the age of the earthquake that offsets the feature is almost always unknown, geologic slip rate studies usually assume that the time between the age of a feature and the initiation of offset of that feature is minimal. The problem of the onset of offset has been noted in previous studies. In examining the San Andreas fault (California, United States), Wallace (1968) implied that the ages of feature formation and feature offset are not identical when he noted that an offset stream channel as we observe it today is a combination of sedimentary and tectonic processes. In a study of the Rodgers Creek-Hayward fault (California, United States), Budding *et al.* (1991) note the potential discordance between the age of channel incision and the age of the earthquake that displaced an offset channel. Budding *et al.* (1991) report a minimum slip rate, given the potential inheritance of a partial earthquake cycle with an unknown length was considered in the slip rate time interval. Dawson and Weldon (2013) note that including open intervals in slip rate calculations could potentially bias slip rates too slowly. To abate this issue, their compilation of California geologic slip rates also includes a generalized “start and end” time of the slip rate, ideally capturing some information over the time interval over which the slip rate is valid. They also note that this potential bias is low if the slip rate interval is long. DuRoss *et al.* (2020) provide a comprehensive treatment of these issues in their study of the Teton fault (Wyoming, United States). To utilize the oldest dated offset available in their study area, DuRoss *et al.* (2020) subtract a characteristic (implied) slip per earthquake from the oldest offset feature (a deglaciation surface). By first subtracting a reasonable amount of displacement from this oldest offset, a closed interval slip rate is then calculated using this feature. Geologic slip rate studies tend to grapple with an extensive determination of the age of the feature, such as wrestling with the possibility of younger terrace riser trimming, for instance (e.g., Ninis *et al.*, 2013), but not precisely with the timing of the earthquake that eventually offset the terrace riser. Not accounting for the age of displacement of a feature is not ignorance; this age determination is simply challenging or impossible without a well-defined and well-dated paleoseismic record likely spanning over 10,000 yr for offset features associated with the Last Glacial Maximum. Many studies recognize the discordance between feature age and age of initial displacement, and report slip rates as minima (e.g., Lee *et al.*,

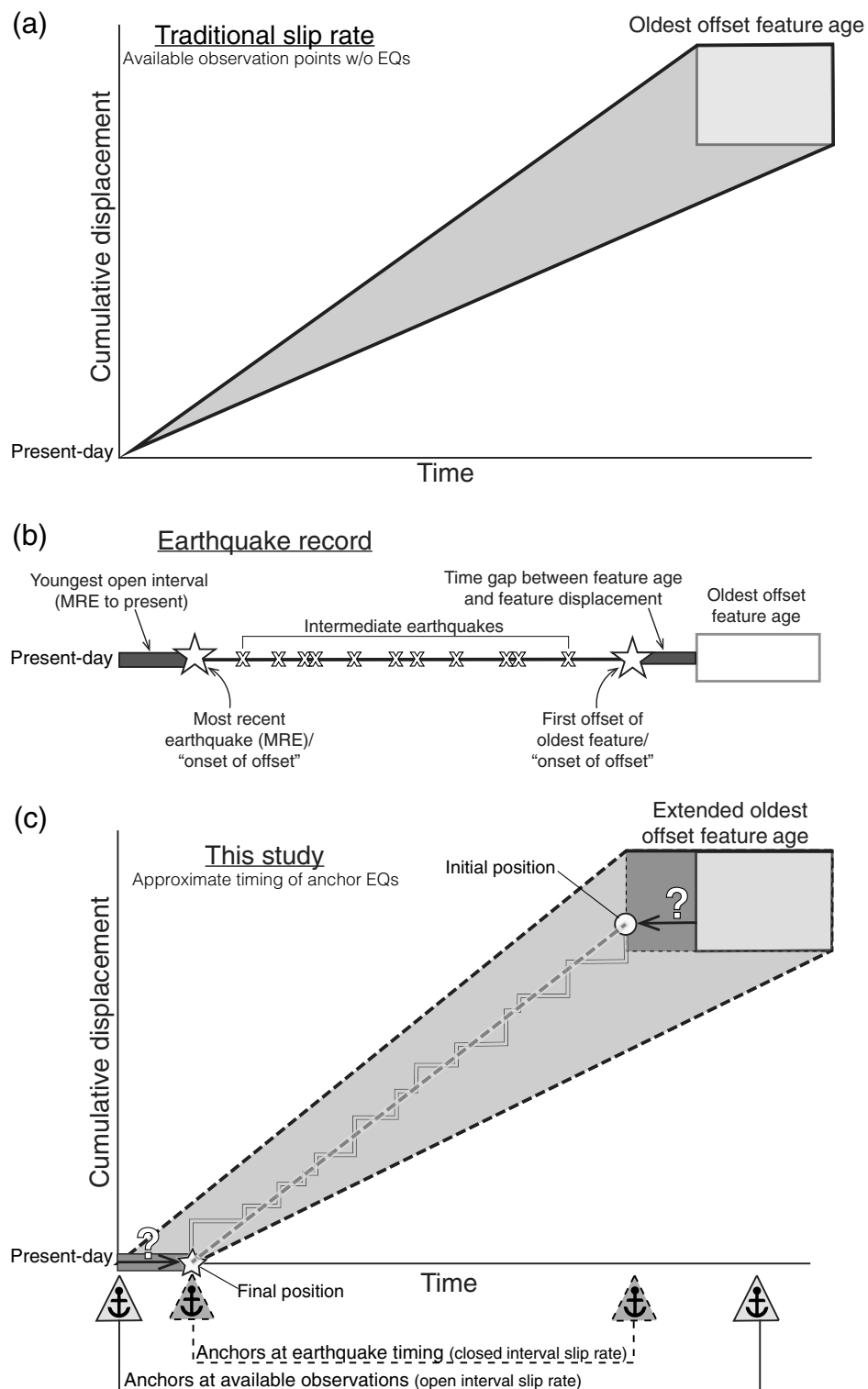


Figure 1. (a) Traditional slip rate formulation using a dated offset feature and the origin of displacement–time space. (b) Schematic timeline of earthquakes through time, with the present day on the left side. Earthquakes of interest that conceptually bound a geologic slip rate are shown with stars. Intermediate earthquakes are shown with x's. The open intervals on either end of the slip rate record are in gray rectangles; the white rectangle shows the age of the oldest offset feature, which is not the age of the earthquake that offsets the feature. (c) Similar to panel (a), with

additions from panel (b), showing our conception of slip rates in this study. The median slip rate is shown as the dashed gray line connecting the white circle (initial position) and white star (final position), calculated after the age of the oldest offset feature is extended younger and present-day is extended older to account for anchor earthquakes. Triangles along the time axis highlight “anchors”—time values that bound a geologic slip rate time interval. Earthquake path shown in light gray stair steps. EQs, earthquakes.

2001; Gold *et al.*, 2015) without further statistical treatment. We extend the mostly qualitative approaches of these prior studies by quantifying the effects of older open intervals on synthetic and published examples of geologic slip rates.

The most recent earthquake and the youngest open interval

Except during the nearly instantaneous occurrence of coseismic slip, fault displacement histories always contain an open interval between the time of the MRE and the present day. Although widely recognized as a problem, accounting for the MRE open interval without knowledge of a paleoseismic or historical earthquake can be vexing in practice. Weldon and Sieh (1985) noted this discrepancy between the origin of displacement–time space (i.e., present-day) and the MRE, and proposed that slip rates be projected to the time of one-half of the average recurrence interval (RI) rather than the present-day. DuRoss *et al.* (2020) calculate numerous slip rates along the Teton fault, including a slip rate anchored at the MRE timing and a displacement-adjusted long-term offset feature, as well as a slip rate anchored at the origin and the oldest offset feature. These preferred slip rates with 1σ errors are 1.1 ± 0.2 mm/yr (projected to MRE) and 0.9 ± 0.06 mm/yr (projected to origin), with the MRE-anchored slip rate nearly 20% faster than the origin-anchored slip rate. In general, problems with including the younger open interval in geologic slip rates are more commonly acknowledged than the older open interval issues.

Our approach

In this study, we test the influence of the onset of offset on geologic slip rate. We refer to the datums that bracket a geologic slip rate time interval as “anchors” (Fig. 1); ideally, these anchors are paleoearthquakes with known timing. However, the precise timing of paleoearthquakes is unknown in most cases, so we expand the concept of anchors to represent probability distributions that approximate the MRE and the initiation of offset of the oldest faulted feature. We use hypothetical and field-observed fault histories along the Wasatch and San Andreas faults to test the influence of various assumptions about the age of slip rate anchors. Because it is usually impossible to determine exactly when faulted features begin to accumulate offset, we leverage constraints provided by intermediate-aged displaced features, along with approximated average RIs, to create probability distributions that account for the possibility that a lag exists between the age of a faulted feature and the onset of faulting.

Open Interval Inheritance as a Function of Recurrence Interval

Defining the problem

The interplay between the number of earthquakes and the length of a displacement record can be schematically visualized as a series of timelines (Fig. 2). As the RI gets longer, so does the potential length of the open interval. On faults with short

RIs (on the order of <1000 yr), open intervals of interest at the start and end of a slip rate record are a relatively small portion of the entire record. However, the problem becomes more pronounced for faults with long RIs (~10,000 yr; Fig. 2b) such that most or all of the slip rate record may be dominated by effects of open intervals at either end of the slip rate record. The time interval over which a geologic slip rate is calculated shortens when open intervals are accounted for (Figs. 1, 2a). The maximum length of open intervals is constrained by intermediate-aged earthquakes. That is, we know open intervals have finite lengths. For example, considering that these analyses concern crustal faults, if a feature is offset 40 m, we can safely assume that more than one earthquake displaced this feature and that multiple intermediate-aged earthquakes contributed to the cumulative offset of this feature.

Figure 3 expands this thinking into time–displacement space. Here, fault histories are depicted as stairs for which each vertical line represents coseismic displacement (i.e., an earthquake). The intervals of interest at each end of the time–displacement record are denoted by thick black lines, which get longer from top to bottom in Figure 3 as RIs increase and slip rates decrease. The intermediate earthquakes that make up the bulk of the time–displacement records in Figure 3 are shown with a thin black line. These earthquake can be modeled as stairsteps to understand nuanced slip rate variability and uncertainty (e.g., Wallace, 1984; Cowie *et al.*, 2012; Styron, 2019; Hatem *et al.*, 2021). However, constraining open intervals is the focus of our analyses, and we ignore the possible variability in time–displacement records, and their accompanying variations in slip rate, that might occur in long records. We discount Figure 3d as a viable slip rate because the slip rate calculated from this earthquake path is composed of a single-earthquake displacement and an unknown portion of two open intervals. Because geologic slip rates are intended to average over multiple earthquakes, a limited record of earthquakes (Fig. 3d) does not achieve the intention of a geologic slip rate. Inherent variability within slip per earthquake over multiple events (or even inherent variability in slip along strike in a single earthquake) and a time interval without a single-closed interval make “one earthquake slip rates,” by definition, not a geologic slip rate because they are not averages of earthquake behavior through time. An average of one sample at a site yields the sample, and that is an observation of paleosurface rupture, not a slip rate.

A potential path forward

With the open interval problem defined, we now explore ways to estimate average geologic slip rates. First, we consider how to best treat the initiation of offset of the oldest faulted feature. In Figure 4, the oldest faulted feature is depicted as a box with a solid black outline in displacement–time space. The earthquake that first offsets the feature can occur anywhere in the box or, importantly, could be younger than the box

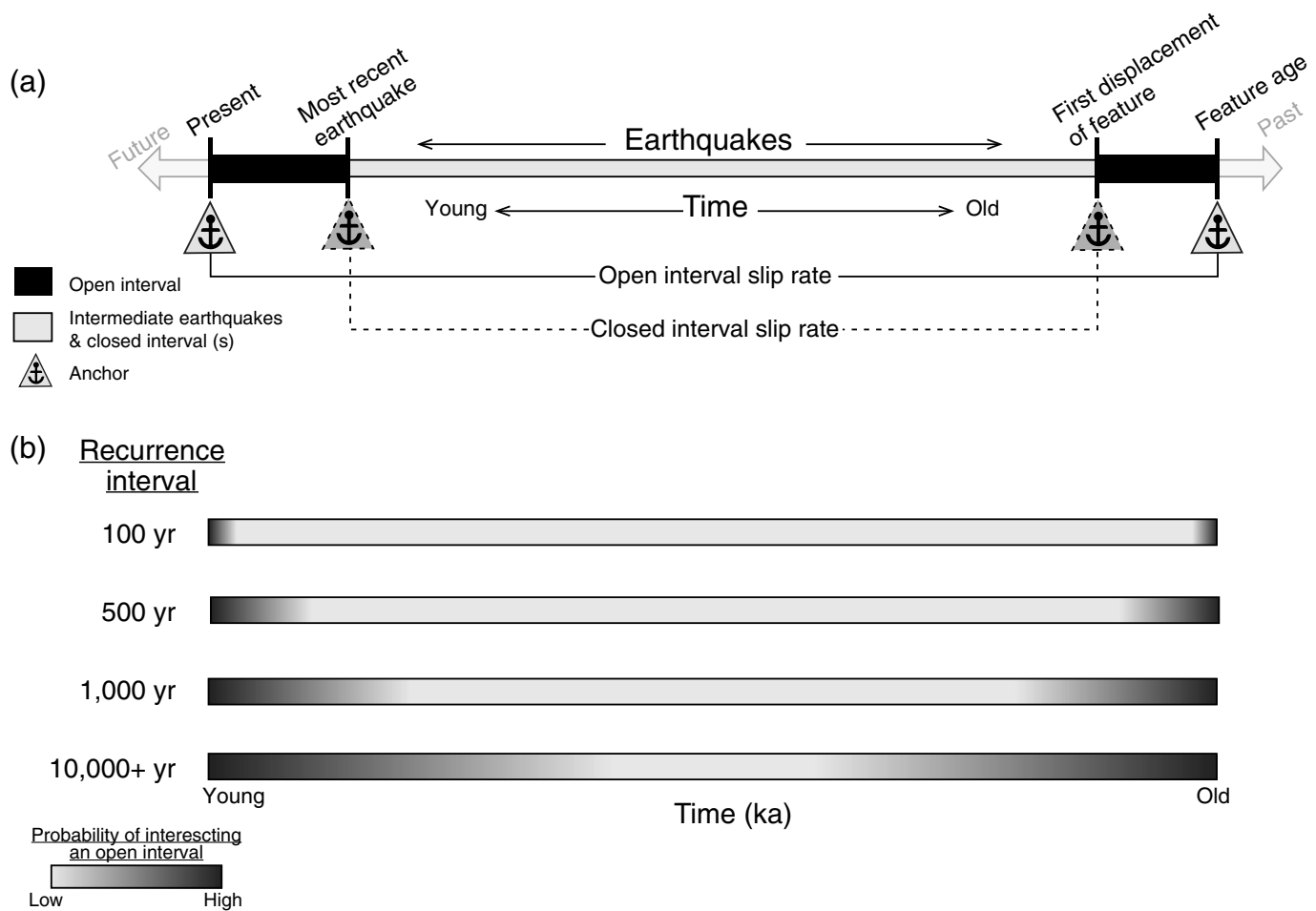


(Fig. 4). To capture the age of the earthquake that first offsets the feature, one could extend the younger edge of the box to encompass the likely range of possibilities. One way is by extending the box by some factor of the average RI in the younging direction (dotted box in Fig. 4). For example, if a fault's RI is roughly 500 yr, a practitioner could extend the minimum age of the oldest offset feature 1000 yr younger ($2 \times$ mean RI as one possibility); this is shown in Figure 4a as a dotted line. If an intermediate feature is present (black dashed box in Fig. 4a), the older edge of the intermediate feature age can be used to reduce the youngest possible age of the extended oldest offset feature. In turn, Figure 4b shows how this treatment can be depicted as a simple triangular probability distribution function.

The MRE open interval can be treated in two ways. The most straightforward way is a direct estimate of the timing of the MRE either known from historical records or determined from paleoseismic records. In the absence of direct knowledge of the timing of the MRE, we can use a probability distribution of likely MRE timing. We outline three options that are based on estimates of average RI (Fig. 4a). The first ("broad MRE") encompasses $2 \times$ the average RI (refer to the Discussion section) and is the most uncertain. The other two options, "young MRE" and "old MRE" in Figure 4a, rely

Figure 2. (a) Generalized timeline with time increasing to the right. Thick black bars show open intervals of interest. Triangles with solid lines show open interval anchors; triangles with dashed lines show closed interval anchors. (b) Timelines are in a similar style as panel (a) schematically plotted for a range of recurrence intervals (RIs) increasing from top to bottom. Black shading indicates a higher probability of sampling an open interval partially bounded by an anchor earthquake, and light gray shading indicates a higher probability to intercept intermediate earthquake and their closed intervals. Transition between black and light gray shading highlights unknown ages of paleoseismic earthquake and uncertainty in the possible length of an open interval.

on the practitioner's best judgment and might be constrained based on the geomorphic expression of faulting (e.g., "young MRE" for fresh scarps and "old MRE" for subdued faulting). Geomorphic expression of scarps can widely vary depending on the climate and precipitation, slip per earthquake, local sedimentology and depositional environments, lithology, and so forth. On top of these complications, average recurrence (e.g., how long a given scarp sits in the landscape) may greatly affect the relative perception of "freshness." Given this subjectivity in MRE age inference, we suggest using the "broad MRE" as opposed to the "young" or "old" MRE approaches in the

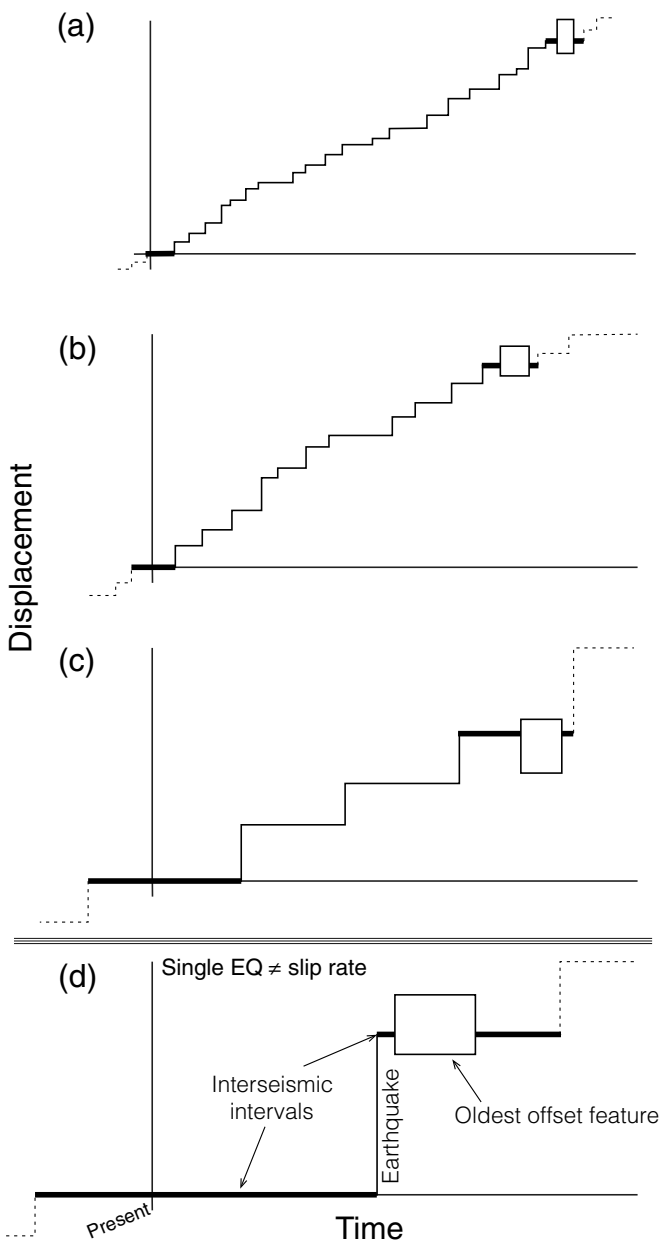


Figure 3. Schematic illustrations of fault histories are represented as stairs with a range of earthquake frequency over the record; RI increases from (a–d) top to bottom. Panel (d) highlights a single-earthquake record and is not a slip rate. Open box represents oldest offset feature. Heavy black lines near the oldest offset feature and the most recent earthquake indicate intervals of interest. Dashed lines on youngest and oldest ends of earthquake path (stairs) represent earthquake cycle continuing beyond the time window of interest.

absence of a paleoseismic MRE age. We later discuss the benefits of using a paleoseismic MRE age over these hypothetical MRE distributions.

A practitioner could use any host of potential distribution choices for feature ages or MRE ages or ways to approximate anchors themselves. In this analysis, we use triangular

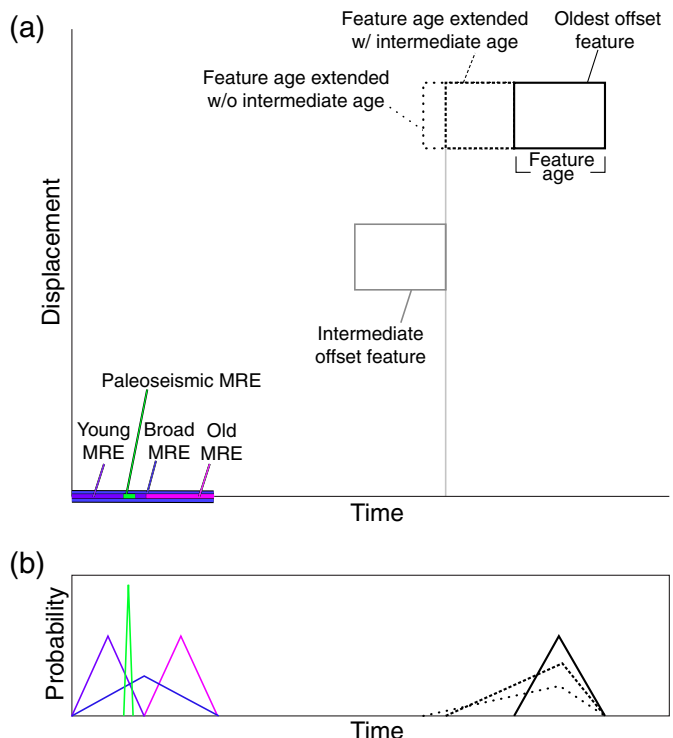


Figure 4. (a) Schematic illustration of various options of anchors explored in subsequent analyses. Solid black box outlines the feature age of the oldest offset feature. The dotted line is extended younger than the offset feature age by some factor. The dashed line and box represent an extended feature age to account for the age of the earthquake trimmed by a younger intermediate feature age. The solid gray box outlines the offset feature of intermediate age. Four possible but nonexhaustive options are shown for the young anchor (most recent earthquake [MRE]): young MRE (purple), old MRE (magenta), broad MRE (blue), and paleoseismic MRE (green). (b) Potential choices for probability density functions (PDFs) as simple triangular distributions. Line colors and styles are the same as (a). The color version of this figure is available only in the electronic edition.

distributions to allow for asymmetric distributions in the case of the extended oldest offset feature and to clearly truncate the edges of the distributions at imposed distribution boundaries. Triangular distributions obviate the need to prescribe more complicated distribution shapes or standard deviation values. Triangular distributions provide a vehicle to express more knowledge than a uniform (boxcar) distribution but are still simpler than a normal distribution or similar. Anchor choice is also clearly variable based on available data or practitioner choice. In our study, for example, MRE anchors are selected as a stepwise increase of additional knowledge and shortening of the time interval assessed. The MRE anchor approximations span the origin (no time range; no additional information), a “broad MRE” (longest time range of 2× generalized RI; acknowledgment of the problem but little additional information), two options to simulate vaguely known MREs as “young” and “old” (shorter time range of 1× generalized RI; potentially

some additional information), and a paleoseismic MRE (narrowest time range of less than a generalized RI; most additional information). These options are meant to be end-member illustrations of possible anchors.

When probability distributions that encompass the oldest and youngest earthquakes in the time–displacement history are defined, we can then calculate slip rates by sampling 10,000 times from these probability density functions (PDFs) for each anchor. We calculate slip rates as a straight line by dividing the cumulative displacement (total offset of the oldest offset feature) by the difference between the old and young anchor picks from the defined distributions. We do not utilize the slip time earthquake paths (STEPS) approach defined in [Hatem et al. \(2021\)](#) because our focus here is an exploration of the influence of open intervals on geologic slip rates. Finally, modeled slip rates are expressed as a distribution (kernel density estimate).

How long can open intervals persist?

Understanding how long an open interval can persist relative to the average earthquake RI—that is, the coefficient of variation—is an open topic of discussion (e.g., [Jackson, 2014](#); [Biasi and Scharer, 2019](#); [Nicol et al., 2024](#)) and is of critical importance for time-dependent probabilistic seismic hazard analyses (e.g., [Weldon et al., 2013](#); [Field et al., 2015](#); [Coffey et al., 2024](#); [Gerstenberger et al., 2024](#)). Although short-time windows of observation may yield apparent hiatuses in earthquake occurrence ([Jackson, 2014](#)), longer histories along, for example, major faults in California, do not yield a similar hiatus ([Biasi and Scharer, 2019](#)). Open intervals along major faults in New Zealand rarely exceed their paleoseismically determined average RI ([Nicol et al., 2024](#)). Clustering of earthquakes (i.e., highly variable RIs) may complicate this factor ([Nicol et al., 2024](#)). Following these studies, we allow for a conservative estimate of a coefficient of variation of 1 in the RI (coefficient of variation = mean/standard deviation; $CV = \sigma/\mu$), which would approach “random” earthquake occurrence (e.g., [Kagan and Jackson, 1991](#)). If we consider a 2σ distribution of RI and wish to maintain a CV of 1, we are led to an open interval estimate of $2\times$ generalized RI.

For the oldest open interval, the onset of offset can be constrained by younger (intermediate) offset features (vertical gray line in Fig. 4a). In the absence of such features, we propose extending the youngest age by a factor of $2\times$ mean RI (dotted box in Fig. 4a). For the MRE open interval, an estimate of the timing of the MRE can also be found using the mean RI. We define the broad MRE as $2\times$ mean RI and young and old MRE as the upper and lower halves of this age range. We provide three simple approaches to generating open interval probability distribution functions here, but alternative models can be constructed. However, the general approach should aim to account for uncertainties in the anchors assigned to slip rate calculations in time–displacement space.

Testing Setup

Synthetic data

We create synthetic fault data across a range of RIs (RI = 150, 400, 1250, and 3000 yr). In these examples, we use a Holocene–latest Pleistocene record with the oldest offset feature spanning 12–15 ka and an intermediate feature with a maximum age of 10 ka (Fig. 5a). At shorter RIs, using the $2\times$ generalized recurrence extension factor, the intermediate aged feature does not intersect the oldest offset feature. Therefore, the intermediate feature cannot trim and reduce the extended age of the oldest offset feature. However, the intermediate offset feature trims the probability distribution function assigned to the oldest offset feature at RI = 1250 and 3000 yr. Triangular distributions describe the probability for each anchor (Fig. 5b). The synthetic dataset allows us to quantitatively explore the influence of RIs with idealized datasets and provide a range of possibilities between the Wasatch and San Andreas fault datasets.

Field data

We use field data from the central Wasatch fault (Utah, United States) and the San Andreas fault (California, United States). The Wasatch fault data include a paleoseismic chronology from the Corner Canyon site ([DuRoss et al., 2018](#); paleoseismic MRE), offsets of an abandoned Lake Bonneville shoreline ([Jewell and Bruhn, 2013](#); oldest offset feature), and a mid-Holocene vertical separation of an alluvial fan ([Personius and Scott, 1992](#); intermediate offset feature; Fig. 6).

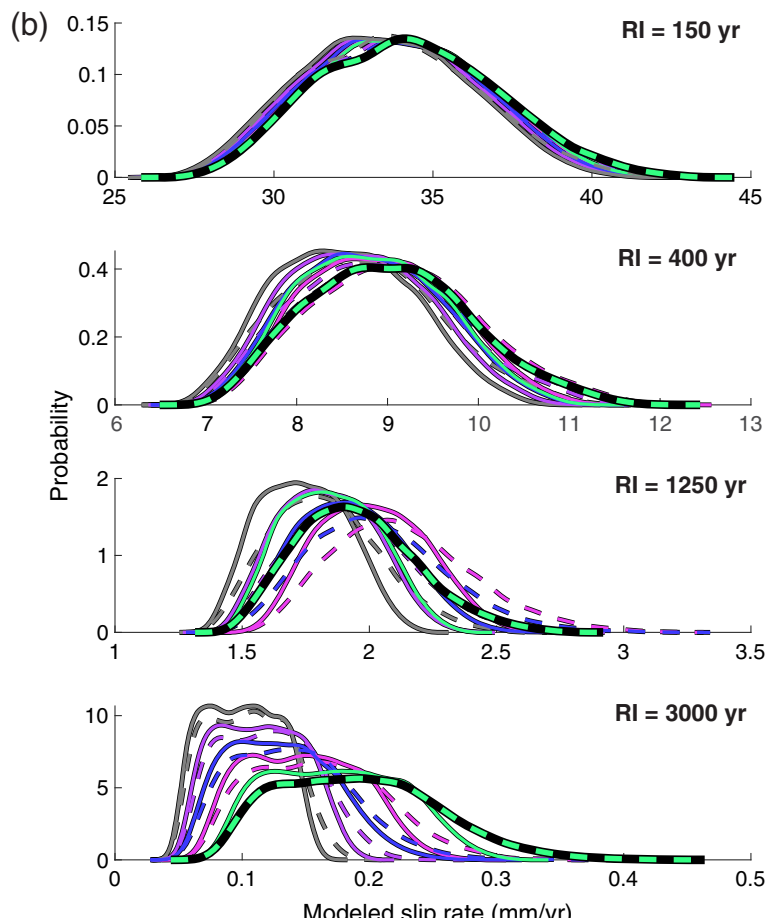
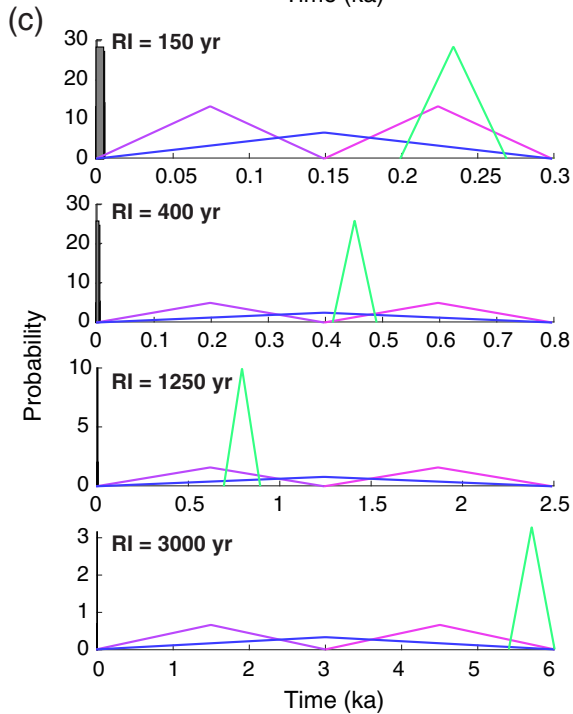
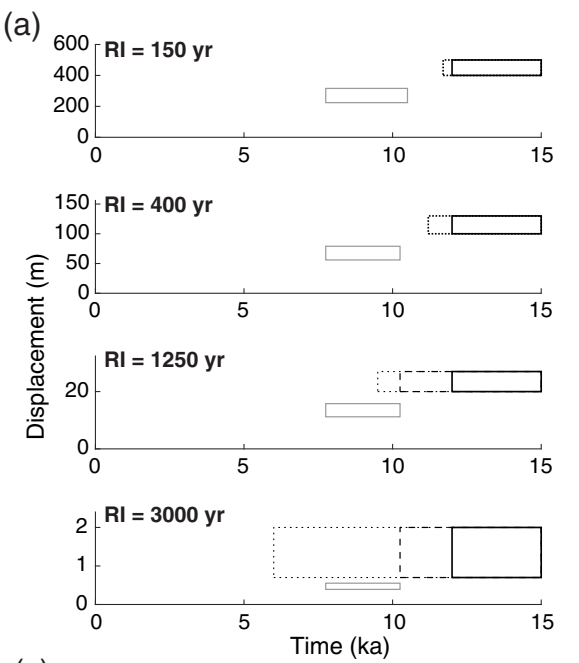
The San Andreas fault data are from the Cajon Creek site near Cajon Pass ([Weldon and Sieh, 1985](#)), and include multiple offset drainages and terrace risers and geomorphic surfaces of intermediate age, as well as a paleoseismic record from a trench virtually collocated with laterally offset features (paleoseismic MRE; Fig. 7). Because we only require the oldest intermediate feature to potentially trim the oldest offset feature of interest in our methodology, we do not discuss the younger intermediate features.

We selected these two field examples as relative end members of a moderate RI fault (Wasatch) and a short RI fault (San Andreas). We test the assertion of [Weldon and Sieh \(1985\)](#) that the influence of the open interval is likely inconsequential on fast-slipping faults such as the San Andreas fault. In contrast to the San Andreas fault, which likely had dozens of earthquakes in the Holocene, the Wasatch fault has \sim 10 earthquakes over the same time interval. These are two of the best-studied faults in the United States and have ample dated offset features and paleoseismic MREs to analyze for this study.

Results

Synthetic data

In the short RI example (RI = 150 yr), all modeled slip rates are roughly equal, and the presence of open intervals does not appear to influence the slip rate (Fig. 5b). At RI = 400 yr, the slip rates using the extended feature age as the old anchor



Preferred closed interval slip rate
(extended feature age to paleoseismic MRE)

Young anchor choice

- Open interval slip rate — Origin
- Approximating closed interval slip rate — Young MRE
- Closed interval slip rate — Old MRE
- Broad MRE

Old anchor choice

- Open interval slip rate — Original feature age
- Approximating closed interval slip rate — Extended feature age

have a longer right-hand tail (faster slip rate) in the modeled slip rate PDF. Using the older MRE for the young anchor extends the right-hand tail the furthest and produces the fastest median slip rate. At RI = 1250 and 3000 yr, the effect of accounting for a wide range of possibilities of the onset of offset is even more pronounced. That is, as the right-hand tail of the modeled slip rate increases, so does the median slip rate. In the RI = 1250 yr case, the median slip rate increases from ~ 1.7 mm/yr in a “traditional” oldest offset feature to origin slip rate to ~ 2.2 mm/yr when the open intervals are accounted for (oldest offset feature-to-older MRE), an increase of $>\sim 25\%$. In

Figure 5. Synthetic data model results. (a) Data setup in displacement-time space. The solid black box represents the oldest offset feature; the dotted black box represents $2 \times$ RI subtracted from the minimum age of the oldest offset feature; the dashed black box represents the extended age of oldest offset feature trimmed by intermediate feature when possible; and solid gray box represents intermediate feature. (b) Kernel density estimates of modeled slip rate PDFs for 10 anchor combinations tested. (c) PDFs for most recent earthquake (MRE) choices. The color version of this figure is available only in the electronic edition.

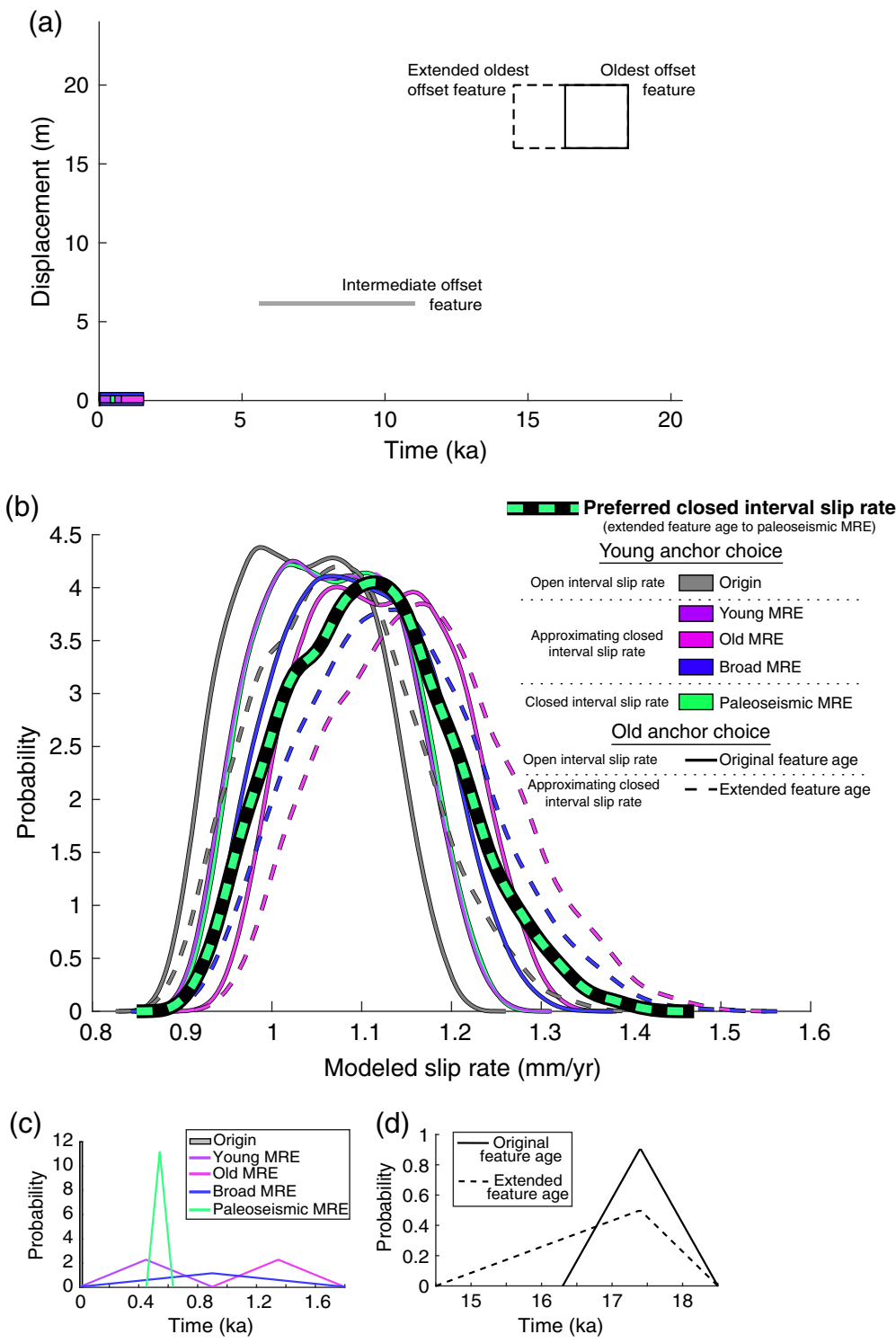


Figure 6. Wasatch fault data setup and results. (a) Data setup in displacement–time space. Paleoseismic chronology and dated offset features from DuRoss *et al.* (2018), Jewell and Bruhn (2013), and Personius and Scott (1992). (b) Modeled slip rate PDFs (kernel density estimate). (c) Young anchor (MRE) PDFs. (d) Old anchor PDFs. The color version of this figure is available only in the electronic edition.

the RI = 3000 yr case, the median open interval slip rate (feature age and origin as anchors) is ~ 0.1 mm/yr. When using the extended oldest offset feature age and the older MRE

modeled time record uses the older MRE and extended feature age as anchors, and here the median slip rate (~ 1.2 mm/yr) increases by $\sim 20\%$ compared to the “traditional” oldest offset

constraints as anchors, the median rate increases to ~ 0.15 mm/yr, representing a $\sim 50\%$ increase in median slip rate depending on the treatment of open intervals. Of note is a possible nonintuitive result; although the paleoseismic MRE spans a smaller temporal range, the modeled slip rate distribution is broad in the case of the RI = 3000 yr. This is because of the heavy right-hand tail; the faster possible rates result from the older paleoseismic MRE and longer RI used in the slip rate calculation. When the paleoseismic MRE is younger (i.e., RI = 1250 yr), the modeled slip rate distribution is narrower and has a similar range as the origin-based slip rates.

Field example: Wasatch fault

The Wasatch fault, with an RI of ~ 900 yr, shows that open intervals in slip rate anchors do influence the modeled geologic slip rate (Fig. 6d). Similar to the hypothetical examples at RI = 1250, the median slip rate and weight of right-hand tails increase as the time record considered between anchors decreases. For example, the slip rate anchored at the feature age and the origin has a nearly symmetric distribution with a median slip rate of ~ 1 mm/yr (gray solid curve in Fig. 6d). When the feature age extended in the young direction to account for the onset of offset is used with the origin as anchors, the median slip rate increases by roughly 15% to ~ 1.15 mm/yr (gray dashed curve in Fig. 6d). The shortest

feature-to-origin anchors (magenta dashed curve in Fig. 6d). Our preferred slip rate uses the paleoseismic MRE and extended feature age as anchors, producing a median slip rate of ~ 1.1 mm/yr (green dashed curve with filled PDF in Fig. 6d). If a range of possible MRE displacement is considered (0.9–1.4 m; DuRoss *et al.*, 2018) in combination with the paleoseismic MRE timing and the extended feature age of the oldest offset feature, the median slip rate decreases from ~ 1.1 to ~ 1.03 mm/yr. Given the intricacies of incorporating per-earthquake displacement into slip rates, we focus on understanding the effect of the onset of offset and not the magnitude of offset itself. In this Wasatch fault example, the MRE is young and exerts a strong constraint on the modeled slip rate. The knowledge of the paleoseismic MRE reduces the possible maximum slip rate (1.2 mm/yr using the “broad” MRE to 1.1 mm/yr with the paleoseismic MRE), reducing the possible underestimate of 20%–10%. In this case, the intermediate offset feature (a dated alluvial fan) does not constrain the onset of offset of the Bonneville shoreline because the age of the intermediate feature is younger than the age of the oldest offset feature extended by a factor of $2\times$ mean RI. The paleoseismic MRE is more useful here for constraining the open intervals than the intermediate offset feature. Our preferred slip rate that approximates closed intervals is ~ 1.1 mm/yr (median value), which matches the slip rates carefully derived by DuRoss *et al.* (2018). The slip rate modeled by DuRoss *et al.* (2018) at Corner Canyon is constrained by the displacement and timing of six paleoearthquakes observed at this site and therefore approximates a closed interval slip rate as we do in this analysis.

Field example: San Andreas fault

Given the relatively short RI of the San Andreas fault as derived by Weldon and Sieh (1985) of ~ 200 yr, the modeled slip rates are not considerably influenced by open intervals. The increase in the modeled median slip rates from open to closed interval slip rates is minimal with about 2 mm/yr over a median slip rate of ~ 25 mm/yr (Fig. 7d). Extending the feature age younger modestly increases the maximum slip rate, slightly drawing out the right-hand tail of the modeled slip rate distribution. Extending the youngest age of the oldest feature overlaps slightly with the oldest intermediate feature dated at Cajon Creek; the oldest age of the intermediate feature is the youngest age of the oldest offset feature (Weldon and Sieh, 1985, Fig. 7a). Without knowing which bounding age is “correct,” we do not use the intermediate feature to trim the extended age of the oldest offset feature. Because of the short, generalized RI of the San Andreas fault, this few centuries-long extension does not greatly influence the resulting slip rates (Fig. 7d). The largest effect on modeled slip rates for the San Andreas comes from the assumption of old or broad MRE, which increases the median modeled slip rate the most compared to the oldest offset feature-to-origin slip rate. Both the old and broad MRE choices allow for long current open intervals, which could

shorten the slip rate time interval the most. This result does not have much meaning because the historical and paleoseismic record of the San Andreas fault is well known. However, this highlights again, as in the Wasatch fault case, that an MRE age is an extremely useful limit on slip rate uncertainty. In this case, modeled median slip rates increase by <10% in the absence of knowledge of the MRE timing.

Our preferred closed interval slip rate in this analysis is ~ 24.9 mm/yr (median value). Again, this compares well to the long-term preferred slip rate modeled by Weldon and Sieh (1985) of 24 mm/yr (difference of $\sim 4\%$). Using multiple markers at the Cajon Creek site, Weldon and Sieh (1985) arrive at a preferred site rate of 24.5 mm/yr. This similarity between our preferred closed interval slip rates and the previously calculated rates highlights the lack of influence of open intervals on fast slipping faults.

Discussion

Which slip rates benefit the most from closed intervals?

The results from a fault with a ~ 900 yr RI (Wasatch fault example) show that the median slip rate could be faster by $\sim 20\%$ depending on the age of the MRE constraint. Reported analytical slip rate uncertainties are in the range of 15%–30% (e.g., 1 ± 0.3 mm/yr); these uncertainties arise from measurement errors in age determination and offset restorations. We show that there may be an unaccounted $\sim 20\%$ underestimate of the geologic slip rate in addition to the 15%–30% analytical uncertainty. Although the minimum rates do not change with these analyses, the maximum rate increases because the probability distributions assigned to the MRE open interval and the onset of offset of the oldest faulted feature shorten the elapsed time of interest.

Taking the western United States as an example, numerous faults fall into this generalized activity category. According to the U.S. Geological Survey (USGS) Quaternary Fault and Fold Database (Haller *et al.*, 1993; U.S. Geological Survey, 2020), faults with generalized slip rates between 0.2 and 5 mm/yr are present throughout the western United States, mainly within Walker Lane, Central Nevada seismic belt, Wasatch front, Yellowstone area, and in the upper plate of the Cascadia subduction zone. In addition, several 0.2–5 mm/yr faults are within the primary North America–Pacific plate boundary zone along the general San Andreas fault corridor. In Figure 8, we highlight the faults with categorical slip rates of 0.2–5 mm/yr according to the USGS Quaternary Fault and Fold Database.

Although these are a small number of affected faults relative to the total inventory of known Quaternary faults across the western United States ($\sim 10\%$ to 15%), it is unknown if the geologic slip rates on these faults are underestimated. Many of these faults are characterized by vertical displacements (on normal faults) on a surface of known or estimated age. For instance, faults that cross a

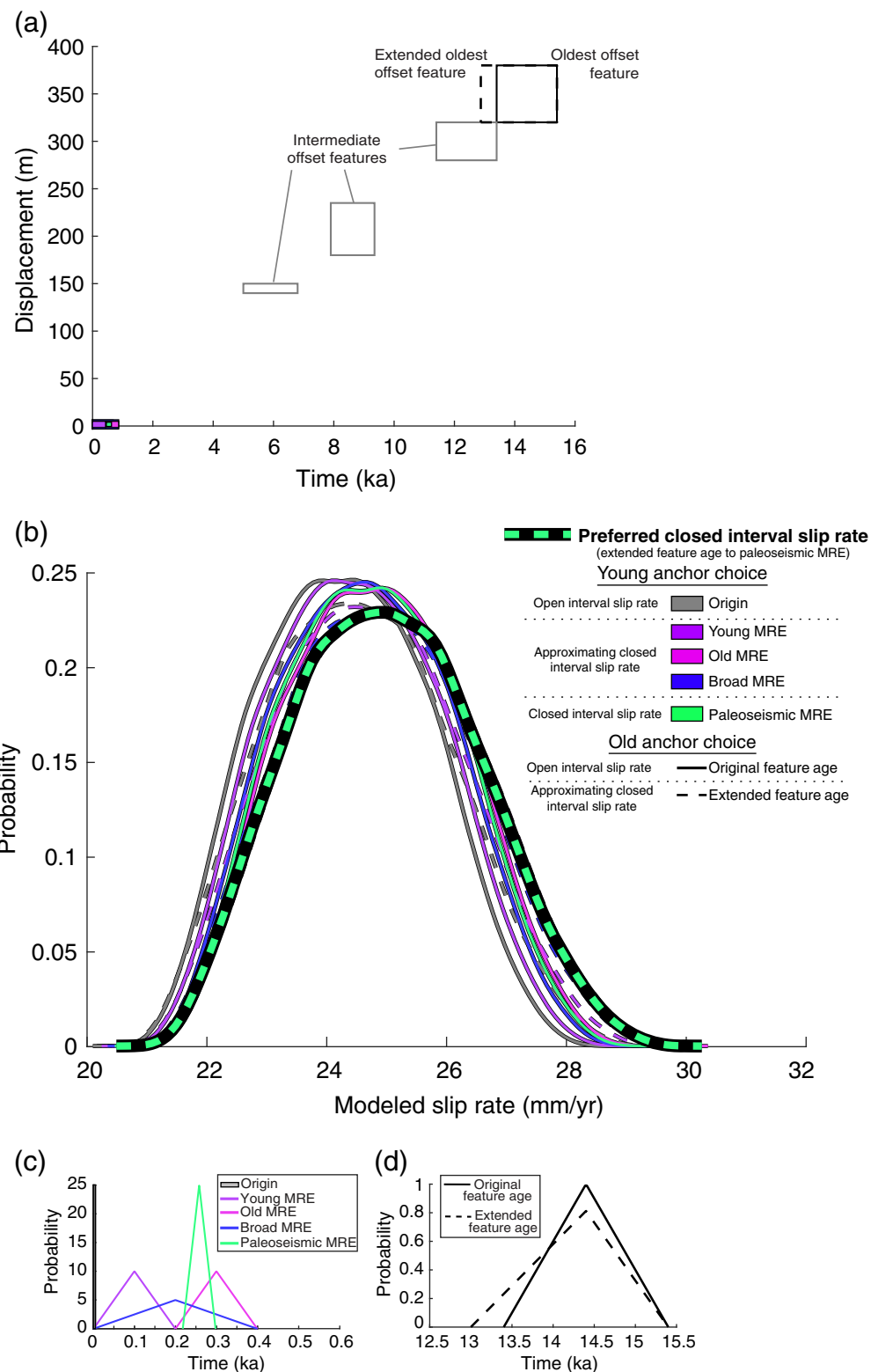


Figure 7. San Andreas fault data setup and results. (a) Data setup in displacement–time space. Paleoseismic chronology and dated offset features from Weldon and Sieh (1985). (b) Modeled slip rate PDFs (kernel density estimate). (c) Young anchor (MRE) PDFs. (d) Old anchor PDFs. The color version of this figure is available only in the electronic edition.

pluvial lake shoreline of known formation (or abandonment) age typically have slip rates calculated with this formation age without much knowledge of the onset of offset of that shoreline. Similarly, many of these faults do not have an MRE estimate to constrain the younger onset of offset. In addition to this proportion of faults characterized by slip rates in the 0.2–5 mm/yr category, even more faults are characterized by slip rates of <0.2 mm/yr. These very slow slip rate faults are all characterized by open interval slip rates of one to two earthquake and would benefit from substantial and systematic reexamination (Fig. 3d).

Further examination of how slip rates are calculated for moderate-rate faults may be important in regions with apparent mismatches between geologic and geodetic moment rates (e.g., Ward, 1998; Pancha *et al.*, 2006). In particular, analysis by Ward (1998) highlights the Basin and Range as a region of considerable discrepancy between geologically and geodetically defined moment rates. Although Ward (1998) suggests that the geologic moment rate may be an underestimate due to unknown faults, this discrepancy may also be due to the geologic slip rate bias illustrated in our study, given that geologic moment rates are based primarily on geologic slip rates and fault-plane area. Subsequent studies have considered similar comparisons with additional (yet still limited) geologic, on-fault data (Pancha *et al.*, 2006), showing that the mismatch between geologic and geodetic moment rate persists with modest additions to the fault

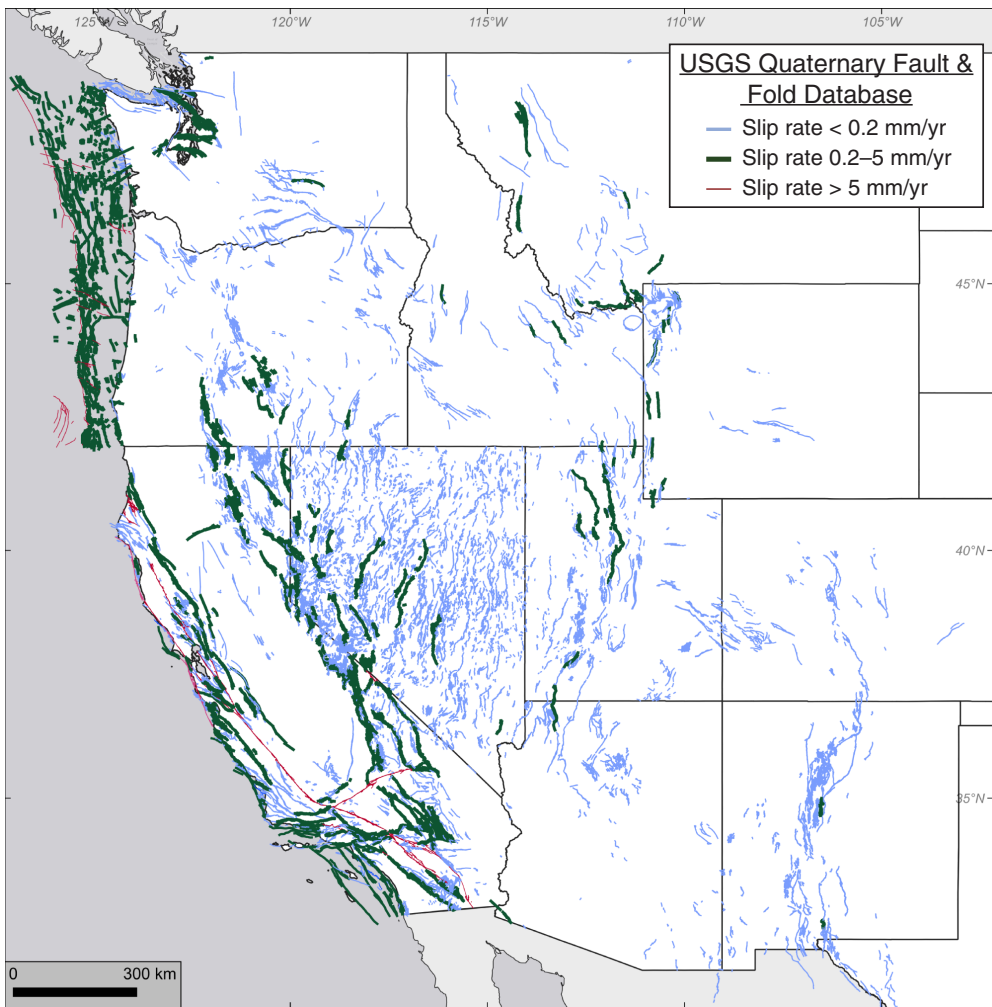


Figure 8. Map of U.S. Geological Survey (USGS) Quaternary Fault and Fold Database across the western United States, highlighting faults with generalized slip rates between 0.2 and 5 mm/yr. The color version of this figure is available only in the electronic edition.

count. Increasing not only the fault count but also the fault-plane area and fault-slip rates may account for a portion of the regional geodetic–geologic moment rate mismatch, particularly in slow to moderately straining regions with undercharacterized faults such as the Basin and Range.

Comparisons to previous work

A previous numerical modeling study by [Styron \(2019\)](#) that tested the effects of seismic cycle variability on slip rates found that slip rate variability decreases substantially after five earthquake cycles. This study also concluded that a slip rate is very stable after about 40 earthquake cycles. Although we do not know exactly how many earthquakes have occurred along the San Andreas fault over the past approximately 14,000 yr, at least 40 earthquakes are plausible (and likely more) in the elapsed time originally documented by [Weldon and Sieh \(1985\)](#) and reanalyzed in our study. Our findings that the geologic slip rate at Cajon Creek is stable without explicitly characterizing the

open intervals within the slip rate agrees well with the findings of [Styron \(2019\)](#). Unlike our study, [Styron \(2019\)](#) held RI constant while testing different distributions to describe recurrence and confirmed that slip rates calculated over a few earthquakes are highly variable compared to the long-term mean. This variability relates to a higher coefficient of variation in recurrence (standard deviation/mean recurrence). In the context of our study, this is due to fewer earthquakes with cumulative geomorphic displacement since the onset of measurable fault displacement (i.e., a longer RI). Our results are consistent with the recommendation of [Styron \(2019\)](#) to propagate uncertainty associated with earthquake cycle effects (such as the open interval influence) with uncertainties in age control and displacement measurements when calculating geologic slip rates.

Implications for probabilistic seismic hazard modeling

The approach we present here may be appropriate for seismic

hazard analyses, especially if all slip rates are treated uniformly. One possibility is to re-evaluate all faults with known or inferred MRE ages to account for the MRE open interval. More ambitious approaches might attempt to recalculate rates using inferred timing of the onset of offset of the oldest offset features used to calculate slip rates. Uniform treatment of slip rates in seismic hazard analyses is key, though, so additional biases are not introduced to deformation models.

Limitations of the methodology

Very few faults have both a paleoseismic record and a slip rate record, presenting a challenge for constraining slip rate with MRE data. Fewer faults have information that can constrain the initiation of offset of the oldest offset feature. Similarly, very few faults have paleoseismic constraints on RI. In the absence of recurrence data, a practitioner could use estimated values of RI with uncertainty distributions and enhance the Monte Carlo sampling scheme presented in this study.

Understanding that the RI of a fault may also be unknown, the use of a generalized (i.e., “categorical” or broad) estimate of RI may suffice. Finally, because this analysis is focused on temporal inheritance and residence time of offset features, we have not provided any treatment of displacement uncertainty itself. Methods for approximating and incorporating the displacement in the anchor earthquakes are not investigated because this work characterizes the influence of earthquake timing on geologic slip rates. Uncertainties in displacement are a fruitful avenue of study and warrant further investigation (e.g., Cowgill, 2007; Reitman *et al.*, 2019).

We have advocated for a multiplier of mean RI to provide a probability distribution for the oldest and youngest anchors used to approximate closed-interval slip rates. However, it may be important to approach this problem in the context of the coefficient of variation of RI for each fault, which we do not do here. More research could help clarify how long an open interval can last, and what factors may influence that open interval length (e.g., regional strain rate, fault length, rake, and spatiotemporal clustering of earthquakes). We recognize that the mean RI only samples the MREs, and more variability could be concealed in the older earthquake record unobserved by paleoseismology.

Recommendations to the earthquake geology community

Based on our analyses, we suggest that, when modeling and reporting slip rates, practitioners: (1) focus on making observations of MRE deformation and modeling MRE timing at a site or generalized along a reach of fault, (2) constrain the mean earthquake RI to provide a basis for creating probability distributions to anchor slip rates, and (3) date intermediate aged offset features in the landscape. All of these parameters can provide better estimates of slip rates than simply dividing the offset of a feature by its age. Constraining the timing of the MRE is the simplest step that can lead to tighter estimates of the geologic slip rate. Although we recognize that not all (or any) of these recommended observations are possible at every slip rate study site, the community can critically consider the biases introduced by traditional slip rate calculations. Furthermore, we recognize that “slip rates” from single-earthquake records (i.e., Fig. 3d) are not representative of multiple earthquakes and are completely controlled by open interval effects. Single-earthquake records are still useful to describe recency and fault activity, but these are not slip rates. Subsequent analyses and models are required to transform these single-earthquake records into longer-term estimates of fault behavior.

Conclusions

We find that geologic slip rates are systematically underestimated if open intervals are not accounted for, particularly in the common approach of dividing the offset of a faulted feature by its age. Slip rates for faults with shorter RIs

($<\sim 1000$ yr) and higher slip rates ($>\sim 5$ mm/yr) are relatively unaffected, but for faults with longer RIs (>1000 yr) and lower slip rates (<5 mm/yr), slip rates can be underestimated by 20% or more. Slip rates along faults with very long RIs ($>\sim 10,000$ yr) are most affected by open intervals, but those issues are not addressable by the methodology in our study. Moderate slip rate faults (~ 0.2 to 5 mm/yr) are particularly susceptible to underestimates of slip rate due to (1) the lag between the formation or abandonment of a feature and onset of offset of faulted features and (2) the common lack of constraints on MRE timing used in slip rate calculations. Slip rates on faster-slipping faults are less susceptible to these issues, but the assumptions are relevant for all faults. We propose a method to calculate slip rates in a way that best approximates a calculation spanning temporally closed intervals by assigning probability distributions to the endpoints of the slip rate calculation. We suggest that providing constraints on the MRE is critical for calculating geologic slip rates and their uncertainty.

Data and Resources

All data used in this article came from published sources listed in the references.

Declaration of Competing Interests

The authors acknowledge that there are no conflicts of interest recorded.

Acknowledgments

The authors thank Sarah Minson for many useful, constructive, and enlightening discussions on these topics. This article greatly benefited from constructive feedback from peer reviewers Rich Koehler, Ashley Streig, and Chris DuRoss.

References

- Biasi, G. P., and K. M. Scharer (2019). The current unlikely earthquake hiatus at California’s transform boundary paleoseismic sites, *Seismol. Res. Lett.* **90**, no. 3, 1168–1176.
- Budding, K. E., D. P. Schwartz, and D. H. Oppenheimer (1991). Slip rate, earthquake recurrence, and seismogenic potential of the Rodgers Creek fault zone, northern California: Initial results, *Geophys. Res. Lett.* **18**, no. 3, 447–450.
- Central and Eastern United States Seismic Source Characterization for Nuclear Facilities (CEUS-SSCn) (2012). Central and Eastern United States seismic source characterization for nuclear facilities, *Technical Rept. EPRI*, U.S. DOE, and U.S. NRC, Palo Alto, California.
- Coffey, G. L., C. Rollins, R. J. Van Dissen, D. A. Rhoades, M. C. Gerstenberger, N. J. Litchfield, and K. K. Thingbaijam (2024). Paleoseismic earthquake recurrence interval derivation for the 2022 revision of the New Zealand National Seismic Hazard Model, *Seismol. Res. Lett.* **95**, no. 1, 78–94.
- Cowgill, E. (2007). Impact of riser reconstructions on estimation of secular variation in rates of strike-slip faulting: Revisiting the Cherchen River site along the Altyn Tagh Fault, NW China, *Earth Planet. Sci. Lett.* **254**, nos. 3/4, 239–255.

- Cowie, P. A., G. P. Roberts, J. M. Bull, and F. Visini (2012). Relationships between fault geometry, slip rate variability, and earthquake recurrence in extensional settings, *Geophys. J. Int.* **189**, no. 1, 143–160.
- Dawson, T. E., and R. Weldon (2013). Appendix B: Geologic slip-rate data and geologic deformation model, *U.S. Geol. Surv. Open-File Rept. 2013-1165-B, and California Geol. Surv. Special Rept. 228-B*.
- DuRoss, C. B., S. E. Bennett, R. W. Briggs, S. F. Personius, R. D. Gold, N. G. Reitman, A. I. Hiscock, and S. A. Mahan (2018). Combining conflicting Bayesian models to develop paleoseismic records: An example from the Wasatch fault zone, Utah, *Bull. Seismol. Soc. Am.* **108**, no. 6, 3180–3201.
- DuRoss, C. B., R. D. Gold, R. W. Briggs, J. E. Delano, D. A. Ostenaas, M. S. Zellman, N. Cholewinski, S. J. Wittke, and S. A. Mahan (2020). Holocene earthquake history and slip rate of the southern Teton fault, Wyoming, USA, *GSA Bull.* **132**, nos. 7/8, 1566–1586.
- Field, E. H., G. P. Biasi, P. Bird, T. E. Dawson, K. R. Felzer, D. D. Jackson, K. M. Johnson, T. H. Jordan, C. Madden, A. J. Michael, et al. (2015). Long-term time-dependent probabilities for the third Uniform California Earthquake Rupture Forecast (UCERF3), *Bull. Seismol. Soc. Am.* **105**, no. 2A, 511–543.
- Gerstenberger, M. C., S. Bora, B. A. Bradley, C. DiCaprio, A. Kaiser, E. F. Manea, A. Nicol, C. Rollins, M. W. Stirling, K. K. Thingbaijam, et al. (2024). The 2022 Aotearoa New Zealand National seismic hazard model: Process, overview, and results, *Bull. Seismol. Soc. Am.* **114**, no. 1, 7–36.
- Gold, P. O., W. M. Behr, D. Rood, W. D. Sharp, T. K. Rockwell, K. Kendrick, and A. Salin (2015). Holocene geologic slip rate for the Banning strand of the southern San Andreas Fault, southern California, *J. Geophys. Res.* **120**, no. 8, 5639–5663.
- Haller, K. M., M. N. Machette, and R. L. Dart (1993). Guidelines for U.S. Database and Map, June 1993, Maps of Major Active Faults, Western Hemisphere International Lithosphere Program (ILP) Project II-2, *U.S. Geol. Surv. Open-File Rept. 93-338*.
- Hatem, A. E., C. M. Collett, R. W. Briggs, R. D. Gold, S. J. Angster, E. H. Field, and P. M. Powers (2022). Simplifying complex fault data for systems-level analysis: Earthquake geology inputs for US NSHM 2023, *Sci. Data* **9**, no. 1, 1–18.
- Hatem, A. E., R. D. Gold, R. W. Briggs, K. M. Shcarer, and E.H. Field (2021). STEPS: Slip time earthquake path simulations applied to the San Andreas and Toe Jam Hill faults to redefine geologic slip rate uncertainty, *Geochem. Geophys. Geosys.* **22**, no. 10, 1–29.
- Jackson, D. (2014). Did someone forget to pay the earthquake bill? *Seismol. Res. Lett.* **85**, 421.
- Jewell, P. W., and R. L. Bruhn (2013). Evaluation of Wasatch fault segmentation and slip rates using Lake Bonneville shorelines, *J. Geophys. Res.* **118**, no. 5, 2528–2543.
- Kagan, Y. Y., and D. D. Jackson (1991). Long-term earthquake clustering, *Geophys. J. Int.* **104**, no. 1, 117–133.
- Lee, J., J. Spencer, and L. Owen (2001). Holocene slip rates along the Owens Valley fault, California: Implications for the recent evolution of the eastern California shear zone, *Geology* **29**, no. 9, 819–822.
- McGill, S., and K. Sieh. (1993). Holocene slip rate of the central Garlock fault in southeastern Searles Valley, California, *J. Geophys. Res.* **98**, no. B8, 14,217–14,231.
- McPhillips, D. (2022). Revised earthquake recurrence intervals in California, USA: New paleoseismic sites and application of event likelihoods, *Bull. Seismol. Soc. Am.* **93**, no. 6, 3009–3023.
- Nicol, A., V. Mouslopoulou, A. Howell, and R. Van Dissen (2024). Why do large earthquakes appear to be rarely “overdue” for Aotearoa New Zealand faults? *Seismol. Res. Lett.* **95**, no. 1, 253–263.
- Ninis, D., T. A. Little, R. J. Van Dissen, N. J. Litchfield, E. G. Smith, N. Wang, U. Rieser, and C. Mark Henderson (2013). Slip rate on the Wellington fault, New Zealand, during the late Quaternary: Evidence for variable slip during the Holocene, *Bull. Seismol. Soc. Am.* **103**, no. 1, 559–579.
- Pancha, A., J. G. Anderson, and C. Kreemer (2006). Comparison of seismic and geodetic scalar moment rates across the Basin and Range Province, *Bull. Seismol. Soc. Am.* **96**, no. 1, 11–32.
- Personius, S. F., and W. E. Scott (1992). Surficial geologic map of the Salt Lake City segment and parts of adjacent segments of the Wasatch fault zone, Davis, Salt Lake, and Utah Counties, Utah, *U.S. Geol. Surv. IMAP 2106*.
- Reitman, N. G., K. J. Mueller, G. E. Tucker, R. D. Gold, R. W. Briggs, and K. R. Barnhart (2019). Offset channels may not accurately record strike-slip fault displacement: Evidence from landscape evolution models, *J. Geophys. Res.* **124**, no. 12, 13427–13451.
- Styron, R. (2019). The impact of earthquake cycle variability on neotectonic and paleoseismic slip rate estimates, *Solid Earth* **10**, no. 1, 15–25.
- U.S. Geological Survey (2020). Quaternary fault and fold database for the nation, doi: [10.5066/P9BCVRCK](https://doi.org/10.5066/P9BCVRCK).
- Wallace, R. E. (1946). A portion of the San Andreas rift in Southern California, *Doctoral Dissertation*, California Institute of Technology, Pasadena, California.
- Wallace, R. E. (1968). Notes on stream channels offset by the San Andreas Fault, southern Coast Ranges, California, *Conf. on Geologic Problems of the San Andreas Fault System*, Stanford University Publication in Geological Sciences, Vol. 11, 6–21.
- Wallace, R. E. (1984). Patterns and timing of late Quaternary faulting in the Great Basin province and relation to some regional tectonic features, *J. Geophys. Res.* **89**, no. B7, 5763–5769.
- Ward, S. N. (1998). On the consistency of earthquake moment rates, geological fault data, and space geodetic strain: The United States, *Geophys. J. Int.* **134**, no. 1, 172–186.
- Weldon, R. J., and K. E. Sieh (1985). Holocene rate of slip and tentative recurrence interval for large earthquakes on the San Andreas fault, Cajon Pass, southern California, *Geol. Soc. Am. Bull.* **96**, no. 6, 793–812.
- Weldon, R. J., T. E. Dawson, G. Biasi, C. Madden, and A. R. Streig (2013). Appendix G: Paleoseismic sites recurrence database, *U.S. Geol. Surv. Open-File Rept. 2013-1165*.

Manuscript received 11 March 2024

Published online 31 July 2024